

# TURBULENCE MEASUREMENTS IN INTERACTING WAKES

**GORDON M. BRAGG and BAILY V. SESHAGIRI\***

Department of Mechanical Engineering, University of Waterloo, Waterloo, Ontario, Canada

(Received 25 August 1972 and in revised form 11 December 1972)

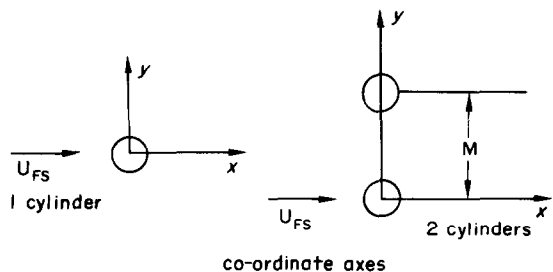
**Abstract**—Detailed measurements of turbulent quantities in the interacting wake of two cylinders have been made. The measurements comprise profiles of mean velocity, turbulent kinetic energy, Reynolds shear stress, intermittency and dissipation in the interacting wake of two equal diameter cylinders, at a number of downstream stations. The diameters of the cylinders as well as the spacing were varied. Simple formulations have been made to predict the distribution of intermittency and turbulent kinetic energy in two cylinder wakes based on measurements in single cylinder wakes. Comparison with measured profiles have proven to be satisfactory. The individual terms of the turbulent kinetic energy equation have been evaluated to present the TKE balance.

The measurements were taken at 87 fps giving a Reynolds number range of from 11 000 to 22 000 (based on the diameter of a single cylinder).

## NOMENCLATURE

$a$ , parameter in equation (6);  
 $d$ , diameter of cylinder;  
 $\text{erf}$ , error function;  
 $I_M$ , total intensity of mean velocity variation =  $\int_{-\infty}^{\infty} (U_{\infty} - U)^2 dy$ ;  
 $I_t$ , total turbulent intensity =  $\int_{-\infty}^{\infty} (\bar{u}^2 + \bar{v}^2 + \bar{w}^2) dy$ ;  
 $K$ , empirical constant in equation (10);  
 $l_k$ , Prandtl-Kolmogorov length scale;  
 $m$ , dummy variable in equations (6) and (9);  
 $M$ , centre to centre spacing between cylinders;  
 $P$ , probability;  
 $p$ , fluctuating component of pressure;  
 $q$ , turbulent kinetic energy (TKE);  
 $R$ , parameter in equation (9);  
 $RN$ , Reynolds number;  
 $S$ , parameter in equation (9);  
 $s$ , parameter in equation (6);  
 $t$ , time;  
 $u, v, w$ , fluctuating components of velocity in  $x, y, z$  directions;

$U, V$ , components of mean velocity in  $x$  and  $y$  directions;  
 $U_{\infty}, U_{FS}$ , free stream velocity;  
 $U_d$ , mean velocity defect =  $U_{\infty} - U$ ;  
 $\bar{uv}$ , Reynolds shear stress;  
 $X$ ,  $x/d$ ;  
 $x_0$ , virtual origin;  
 $Y$ ,  $y/d$ ;  
 $Y(t)$ , instantaneous position of boundary separating turbulent and non-turbulent flows;  
 $x, y, z$ , cartesian coordinates axis,  $x$  in the direction of the free stream,  $z$  along axis of cylinder,  $y$  perpendicular to  $x$  and  $z$ ;  
 $\bar{Y}$ , mean position of  $Y(t)$



\* Present address: Institute for Aerospace Studies, University of Toronto, Toronto 5, Ontario.

## Greek symbols

$\gamma$ ,	intermittency factor;
$\varepsilon$ ,	rate of turbulent dissipation;
$\lambda$ ,	micro or dissipation scale;
$\mu_{\text{eff}}$ ,	eddy viscosity;
$\nu$ ,	kinematic viscosity;
$\rho$ ,	density;
$\sigma$ ,	standard deviation of the distortion $Y$ from its mean $\bar{Y}$ ;
$\tau$ ,	shear stress;

An overbar indicates time averaging. Subscripts 1 and 2 refer to cylinders 1 and 2.

## 1. INTRODUCTION

INTERACTING shear flows occur in a variety of practical flow situations. Exhausts from multiple jet engines of aircraft which expand downstream and interact with each other is one example. Another example is the flow past banks of tubes in boilers and heat exchangers whose individual wakes expand and interact with each other to form a combined wake. The present work was undertaken to study certain aspects of one such flow.

The flow considered was the two dimensional, subsonic, incompressible, interacting far wake behind two equal diameter cylinders. Gran Olsson [1] measured mean velocity and temperature profiles in the wakes of arrays of cylinders. He also gave an analytical solution for the mean velocity profile in such wakes based on Prandtl's mixing length hypothesis. Tamaki and Oshima [2] and Sato [3] have reported experimental studies behind a row of heated rods.

Stewart [4] conducted experiments in the wake of arrays of cylinders. Although he was more interested in examining the wake far downstream, where there are no significant mean velocity gradients, he reported data on the decay of mean velocity and TKE. He was the first to point out the main difference between single cylinder wakes and interacting wakes. In single cylinder wakes, sufficiently far from the body, an equilibrium situation will be established

wherein the rate of production of turbulence will be approximately equal to the rate at which the flow is losing TKE due to viscosity. In interacting wakes such an equilibrium is never established due to the fact that the wake dimensions cannot expand laterally. This causes the mean stream variation to disappear rapidly. Expressing this mathematically, defining

$$I_m = \int_{-\infty}^{\infty} (U_x - U)^2 dy$$

and

$$I_t = \int_{-\infty}^{\infty} (\bar{u}^2 + \bar{v}^2 + \bar{w}^2) dy,$$

in the one cylinder case,  $I_m/I_t$  reaches an asymptotic value of about two whereas in the interacting wake this ratio tends to zero. This points out the essential non-equilibrium nature of the flow.

Knystautas [5] has reported measurements in turbulent jets emitted from a series of holes in line. Champagne and Wygnanski [6] have reported an experimental investigation of coaxial turbulent jets. They have published extensive measurements of mean velocities, turbulence intensities, and shear stresses in two coaxial jets.

## 2. BASIC EQUATIONS AND QUANTITIES MEASURED

The equations which describe the flow field in a 2-dimensional wake can be derived from the Navier-Stokes equation based on boundary layer type approximations [7, 8]. The basic equations are:

Momentum

$$U \frac{\partial U}{\partial x} + V \frac{\partial U}{\partial y} = \frac{\partial}{\partial y} \left( \nu \frac{\partial U}{\partial y} - \bar{uw} \right) \quad (1)$$

Turbulent Kinetic Energy

$$U \frac{\partial \bar{q}^2}{\partial x} + V \frac{\partial \bar{q}^2}{\partial y} = -\bar{uw} \frac{\partial U}{\partial y} - \frac{\partial}{\partial y} \overline{v \left( \frac{p}{\rho} + q^2 \right)} - \varepsilon \quad (2)$$

## Continuity

$$\frac{\partial U}{\partial x} + \frac{\partial V}{\partial y} = 0 \quad (3)$$

The physical interpretation of the various terms is well known [7, 8].

The following quantities were measured:

- (a)  $U$  component of mean velocity
- (b) Turbulent kinetic energy ( $u, v, w$  components)
- (c) Reynolds shear stress ( $\overline{uv}$ )
- (d) Dissipation ( $\epsilon$ )
- (e) Intermittency factor ( $\gamma$ )

Intermittency which does not appear in the basic equations explicitly, is recognized as playing an important role in turbulent shear flows.

## 3. EXPERIMENTAL DETAILS

The experiments were conducted in the open circuit wind tunnel in the Department of

Mechanical Engineering, University of Waterloo. The test section was 2 ft wide, by 3 ft high and 6 ft long. The contraction ratio was 9.2 to 1. The turbulent intensity ( $\sqrt{\overline{u^2}}/U$ ) in the test section was about 0.15 per cent. The maximum attainable wind speed was about 200 fps. The tests were conducted at about 87 fps. The pressure gradient along the test section was negligible in a momentum balance. The wake producing cylinders spanned the entire width of the tunnel. They were commercially available lengths of aluminium rods. A permanently mounted pitot-static tube allowed the free stream velocity to be monitored at all times. It was also used to linearize and calibrate the hot wire anemometer.

Most of the electronics used consisted of DISA units including the DISA 55D01 constant temperature anemometer, DISA 55D10 linearizer, etc. The DISA 55A06 Random Signal

Table 1. Range of measurement of intermittency factor, mean velocity, turbulent kinetic energy, and shear stress (cylinder diameter = 0.5 in.)

$n$	$M$ (in.)	$x$ (in.)	$M/d$	$x/d$	$x/M$
1	—	20.5	—	41	—
2	5		10		4.1
	5.5		11		3.72
	6		12		3.42
	6.5		13		3.15
1	—	25.75	—	51.5	—
2	5		10		5.15
	5.5		11		4.68
	6		12		4.29
	6.5		13		3.96
	7		14		3.68
1	—	32.25	—	64.5	—
2	5		10		6.45
	5.5		11		5.86
	6		12		5.37
	6.5		13		4.96
	7		14		4.6
1	—	40.75	—	81.5	—
2	5		10		8.15
	5.5		11		7.41
	6		12		6.8
	6.5		13		6.27
	7		14		5.83

## Symbols

$n$ —no. of cylinders;  $M$ —spacing between cylinders;

$x$ —distance downstream from plane of cylinders;  $d$ —diameter of cylinders.

Table 2. Range of measurement of intermittency factor, mean velocity, turbulent kinetic energy, and shear stress (diameter of cylinder = 0.25 in.)

<i>n</i>	<i>M</i> (in.)	<i>x</i> (in.)	<i>M/d</i>	<i>x/d</i>	<i>x/M</i>
2	2.5	20.5	10	82	8.2
	3		12		6.83
	3.5		14		5.85
	4		16		5.12
2	2.5	25.75	10	103	10.3
	3		12		8.58
	3.5		14		7.35
	4		16		6.44
2	2.5	32.25	10	129	12.9
	3		12		10.75
	3.5		14		9.2
	4		16		8.06
4.5	18	7.16			
1	—	40.75	—	163	—
2	2.5		10		16.3
	3		10		13.58
	3.5		14		11.62
	4	16	10.18		
4.5	18	9.05			

Table 3. Range of measurement of turbulent dissipation

<i>n</i>	<i>d</i> (in.)	<i>M</i> (in.)	<i>x</i> (in.)	<i>M/d</i>	<i>x/d</i>	<i>x/M</i>
1	0.5	—	20.5	—	41	—
1	0.25	—		—	82	—
2	0.5	5	40.75	10	41	4.1
	0.5	6		12	41	3.42
	0.25	2.5		10	82	8.2
	0.25	3.5		14	82	5.85
1	0.5	—	40.75	—	81.5	—
1	0.25	—		—	163	—
2	0.5	5		10	81.5	8.15
	0.5	6		12	81.5	6.8
	0.25	2.5	10	163	16.3	
	0.25	3.5	14	163	11.63	

Indicator and Correlator which has a built in differentiating circuit was used in the measurement of dissipation. Other circuits like the summing and differencing circuit, integrator, Schmidt trigger, etc., were built using Philbrick Operational Manifolds.

The diameter of the rods tested were 0.25 in. and 0.5 in. The *RN* based on rod diameter ranged from 11 000 to 22 000. Tables 1, 2 and 3 show the complete range of tests conducted.

Although most of the measurements were straightforward, some difficulty was encountered

in the measurement of dissipation and intermittency. These will be briefly discussed below. Turbulent dissipation was measured by making use of the concept of local isotropy and Taylor's hypothesis. With these assumptions the expression for  $\epsilon$  becomes:

$$\epsilon = \frac{15\nu}{U^2} \left( \frac{du}{dt} \right)^2 \quad (4)$$

(see References [7] or [8] for details).

The difficulty is due to two main reasons.

Firstly, the flow is nonisotropic. This can be seen from Fig. 2 where the three components of turbulent intensity have been plotted. As a consequence of this anisotropy, the validity of equation (4) is open to question. However, this approximation is of necessity in common usage. The second difficulty arose due to the inherent noise of the differentiating circuit. To overcome this problem, a low pass filter of 10 kHz was used. To give an indication of the effect of the filter, two tests were run under identical conditions in all respects except that in one run the low pass filter was set at 10 kHz and in the other at 5 kHz. The results are shown in Fig. 1.

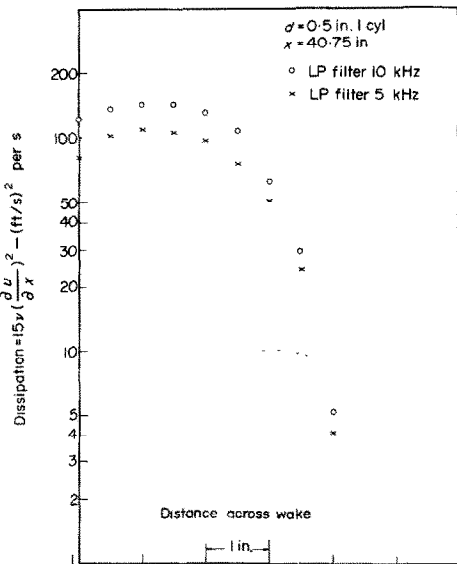


FIG. 1. Effect of LP filter setting on the measurement of dissipation.

It is seen that the 5 kHz filter reduces the measured dissipation by a factor of about 1.36. Bradbury [9] encountered the same problem in his measurements in a jet. He also found that in a jet the frequency of the eddies could extend beyond 15 kHz. To overcome the difficulty, it was decided to use the LP filter at 10 kHz and suitably scale the measured dissipation so as to

satisfy the TKE balance. This was also the procedure followed by Bradbury [9]. The average value of this scaling factor came to 3.75 in the present case. Bradbury (who used a filter setting of 15 kHz) reports a value of 2. Kacker and Whitelaw [10] had the same difficulty and their factors ranged from 1.3 to 4.0.

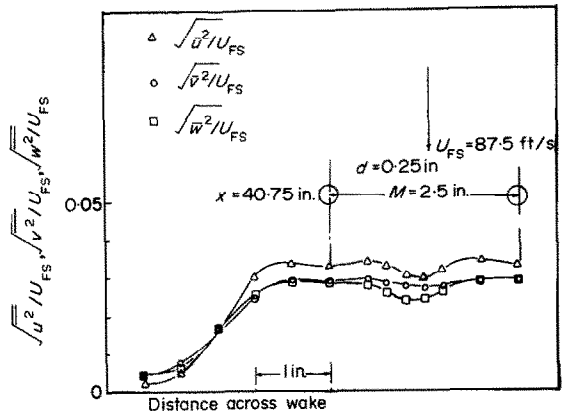


FIG. 2. Components of turbulent intensity across 2 cylinder wake.

A slightly modified version of the circuit used by Corrsin and Kistler [11] was used to measure the intermittency factor,  $\gamma$ . This involved filtering the HW signal, amplifying it, rectifying it, passing it through a Schmidt trigger, integrating the output of the trigger for a known duration of time, and measuring the integrator output with a DVM. The trigger has an output only so long as the input exceeds a certain preset threshold value. If the input falls below this value, the trigger output will be zero. Hence this output is proportional to  $\gamma$ .

The difficulty with the above circuit was in choosing the proper threshold level and "memory" time. The method used in the present case was to display the HW output on an oscilloscope with storage facility and photograph it. By actually measuring the duration of turbulent bursts one could evaluate  $\gamma$  and thus calibrate the circuit. Details of this problem are discussed in Seshagiri and Bragg [12].

#### 4. DISCUSSION AND RESULTS

Experimental data for the 0.25 in. dia cylinders will be presented here. The graphs for  $d = 0.5$  in. are similar and are omitted for the sake of brevity. However they will be used for discussion of results. Detailed results of the measurements can be found in Seshagiri [13]. Measurements of the mean velocity profiles in the wakes of cylinders of equal as well as unequal diameters and spacings have been reported, and wake width variation with distance discussed, in Bragg *et al.* [14] and will not be discussed here.

##### Intermittency measurements

From the work of Townsend [8] has emerged the picture of the dual structure of the wake, consisting of large scale eddies superimposed on eddies of smaller scale.

intermittency factor in the interacting wake of two cylinders based on measurements in the wake of a single cylinder.

By definition, intermittency factor  $\gamma(y)$ , is the probability that at any point in the wake the flow is turbulent. For the range of  $x/d$  considered in the present investigation (up to  $x/d \approx 160$ ) it was observed that the flow along the centre line of the cylinder was fully turbulent all of the time. Consequently,  $\gamma$  can be assumed to be 1 along the centreline. As we move away from the centreline towards the edge of the wake, the probability of turbulence being present reduces, tending to zero. If the probability of event A occurring is  $P(A)$  and the probability of event B occurring is  $P(B)$ , the probability of either A or B occurring is,

$$P(A \text{ or } B) = P(A) + P(B) - P(A \text{ and } B).$$

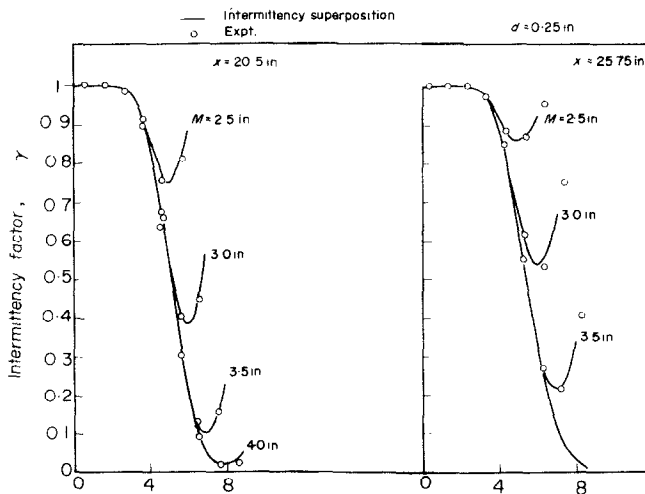


FIG. 3. Intermittency factor profiles.

The larger scale eddies are the ones responsible for the intermittent nature of the wake. According to Grant [15], the large scale motion consists of jets of fluid billowing or erupting from the core of the wake into the undisturbed fluid. The jets are probably produced by pressure fluctuations within the core. With this physical picture in mind, an attempt was made to predict the

If the events A and B are independent of each other,

$$P(A \text{ and } B) = P(A) \cdot P(B).$$

Consequently,

$$P(A \text{ or } B) = P(A) + P(B) - P(A) \cdot P(B).$$

On this basis, intermittency has been superposed:

$$\gamma(y) = \gamma_1(y) + \gamma_2(y) - \gamma_1(y)\gamma_2(y) \quad (5)$$

where  $\gamma_1(y)$  is the intermittency at some point  $y$  due to cylinder 1 alone,  $\gamma_2(y)$  is the intermittency at the same point due to cylinder 2 alone and  $\gamma(y)$  is the resultant intermittency at that point due to the presence of both the cylinders.

The above calculation was carried out and the results are shown in Figs. 3 and 4 which also

the velocity of the jets is small, they are likely to diffuse into each other and ultimately fall back without folding as they do in a single cylinder wake.

From a knowledge of intermittency it is possible to get an idea of the rate at which turbulence is encroaching upon the undisturbed fluid. Townsend [8] has noted that the profiles of intermittency can be represented by an error

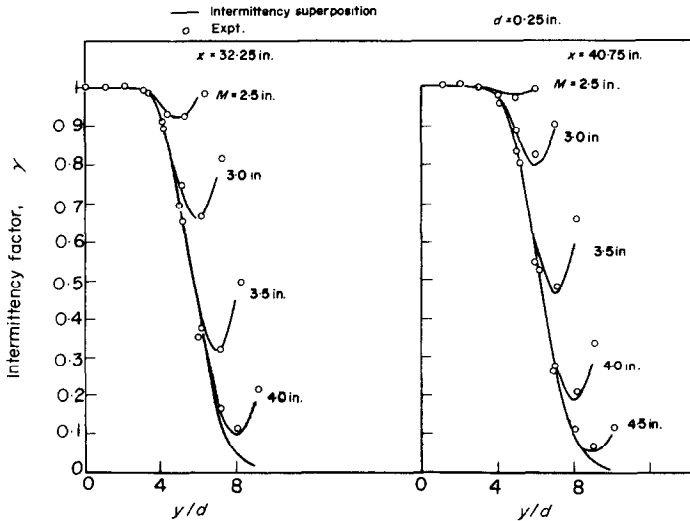


FIG. 4. Intermittency factor profiles.

have the experimentally measured points plotted on them. The comparison is seen to be satisfactory. The same agreement held for the  $\frac{1}{2}$  in. dia cylinders as well. At low values of  $\gamma$  this is not surprising, i.e. at distances where the wakes have just started to interact, one would expect the intermittency to be the sum of the intermittencies due to each of the cylinders.

It would be of interest to know what happens to the jets of erupting fluid (as proposed by Grant) if they do coincide. This would be a Lagrangian problem and difficult to measure. A conjuncture could be made based on Townsend's hypothesis regarding these jets. Since they are basically moving outward, they have velocities in opposite directions. However, since

function of the form

$$\gamma(y) = \frac{1}{\sqrt{2\pi}} \int_{(y/s)-a}^{\infty} e^{-m^2/2} dm \quad (6)$$

where  $s$  and  $a$  are parameters which can be varied to give the best fit.  $\gamma(y)$  can be defined as

$$\gamma(y) = \text{Prob} [y < Y(t)]$$

where  $Y(t)$  is the instantaneous position of the boundary separating the turbulent and non-turbulent fluids. The probability density  $P(y)$  of  $Y(t)$  is defined as  $-d\gamma/dy$ . The standard deviation  $\sigma$  of  $P(y)$  is a measure of the distortion of  $Y$  from its mean position

$$\sigma^2 = \int_{-\infty}^{\infty} P(y)(y - \bar{Y})^2 dy \quad (7)$$

where

$$S = \gamma(M/2), R = 1 - S.$$

where

$$\int_{-\infty}^{\infty} P(y) (y - \bar{Y}) dy = 0 \text{ defines } \bar{Y} \quad (8)$$

with these definitions it can be shown from (6), that  $\sigma^2 = s^2$  and  $\bar{Y} = as$ . The variation of  $\sigma$  with  $x$  gives an indication of the rate of encroachment of turbulent fluid into nonturbulent fluid.

Equation (6) can be fitted to the single cylinder cases. For the two cylinder cases equation (6) has to be modified slightly. The error function as used in equation (6) varies between the limits 0 and 1, i.e. when  $y \rightarrow 0$ ,  $\text{erf}(y) \rightarrow 1$  and when  $y \rightarrow \infty$ ,  $\text{erf}(y) \rightarrow 0$ . For the two cylinder case,

By placing  $S = 1$ , equations (9) and (6) become identical. The results of fitting equation (9) to the measured data are shown in Figs. 5 and 6. The results are satisfactory. The same was true for the  $\frac{1}{2}$  in. dia cylinders.

Figure 7 shows  $\sigma$  plotted against  $x$  for the single cylinder case and  $1 - \sigma$  plotted against  $x$  for the two cylinder cases. The reason for plotting  $1 - \sigma$  rather than  $\sigma$ , as in the one cylinder case, is as follows. In the latter case, the wake spreads and as the turbulent fluid encroaches on the nonturbulent fluid, the excursions of the boundary from the mean increases thus increasing  $\sigma$ .

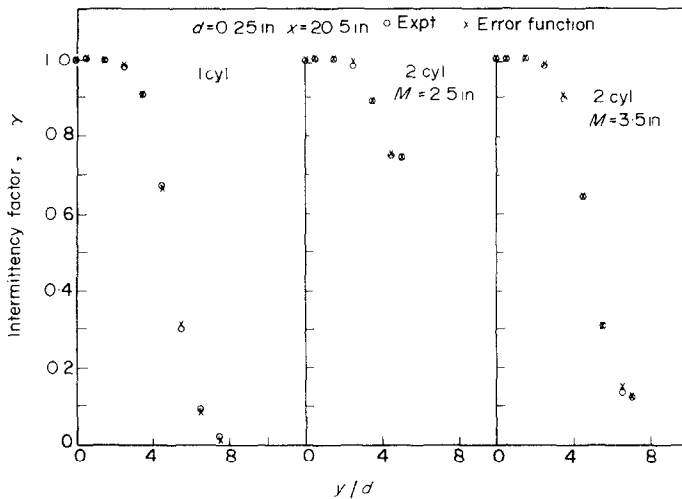


FIG. 5. Error function fitted to intermittency profiles.

due to wake interaction,  $\gamma(y)$  does not tend to zero. It reaches a minimum at  $y = M/2$  and then increases again. To accommodate this behaviour, the following function was used

$$\gamma(y) = R + \frac{S}{\sqrt{2\pi}} \int_{(y/s)-a}^{\infty} e^{-m^2/2} dm \quad (9)$$

For the two cylinder case as we proceed downstream,  $\gamma$  will become one throughout the cross-section between the cylinders. This will mean that  $\sigma$  will tend to zero. Consequently the reduction of  $\sigma$  or the increase of  $1 - \sigma$  indicates the conversion of nonturbulent or partially turbulent fluid into fully turbulent fluid. Due to the limited number of points available it is



difficult to draw conclusions as to the specific rates of encroachment. In the two cylinder case the process should be viewed more as transferring momentum within the confines of the cylinders

wakes show that only in a very narrow zone is the distribution affected by interaction. This becomes clearer when one considers the intermittency and the TKE distribution behind the

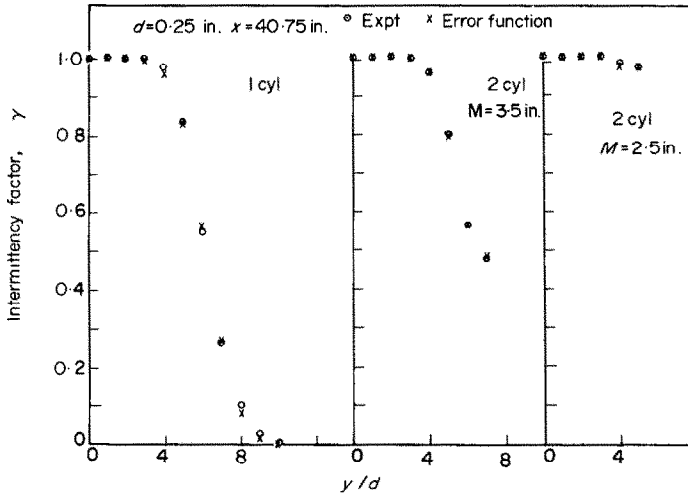


FIG. 6. Error function fitted to intermittency profiles.

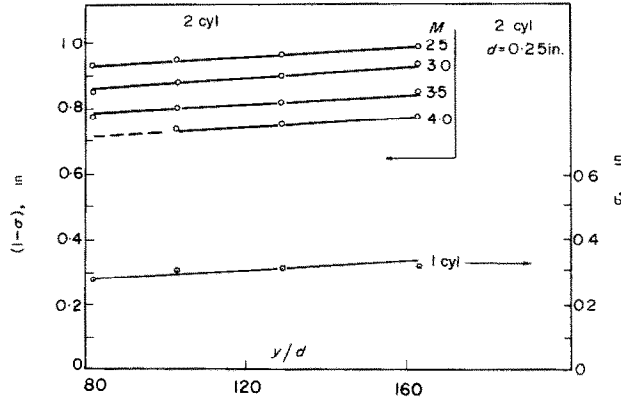


FIG. 7. Spread of turbulent front.

rather than entrainment of free stream momentum as in the one cylinder case.

*Turbulent kinetic energy measurements*

Until one goes a considerable distance downstream, the TKE distribution in the two cylinder

$\frac{1}{4}$  in. dia cylinder at  $x = 20.5$  in.,  $M = 3$  in. At the mid point between the cylinders,  $\gamma \approx 0.4$  whereas the TKE is only 7 per cent of its value at  $y = 0$ . This points out the low energy content of the large scale eddies which would be essentially responsible for the interaction until

one goes sufficiently far downstream. Another feature is that the  $\gamma$  distribution becomes one throughout the interacting layer much faster than the TKE distribution. While the variation in the  $\gamma$  profile is smoothed out at  $x/M \approx 17$ , one has to go to  $x/M \approx 30$  to smooth out the variations in the TKE profile.

Bragg *et al.* [14] have shown that momentum can be superposed to calculate the mean velocity profile in the wake of multiple cylinders based on that of single cylinders. In an analogous manner, the superposition of TKE was attempted with the view of predicting the TKE profiles in interacting wakes based on measurements in

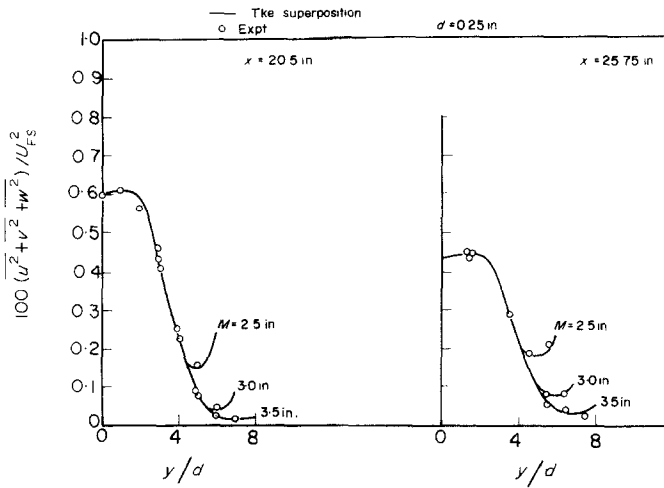


FIG. 8. TKE profiles.

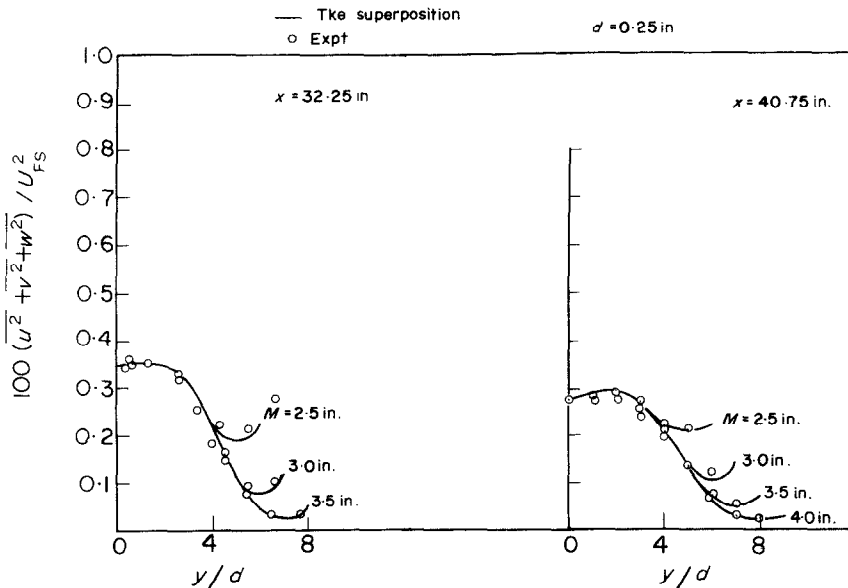


FIG. 9. TKE profiles.

single wakes. The argument in this case is also simple. At low intermittencies, the TKE due to each of the cylinders will be nearly additive due to the low probability of interaction. At higher intermittencies, i.e. where wake interaction has proceeded to a considerable degree, more of the jets will interact and since they frequently have velocities in opposing directions, will tend to reduce the total TKE. One simple relationship which would satisfy the requirements is

$$q(y) = [q_1(y) + q_2(y)][1 - K\gamma_1(y)\gamma_2(y)] \quad (10)$$

subscripts 1 and 2 refer to values with only one cylinder present.  $K$  is an arbitrary constant. For the above relationship to have any use,  $K$  should be a universal constant, i.e. it should be the same at least for different Reynolds numbers. The value of  $K$  was determined using the measured values at one particular location for a single cylinder as well as for two cylinders. The value thus found was 0.274. This value was not altered for all other calculations.

The results of the above calculation are shown in Figs. 8 and 9. The agreement is satisfactory. The same sort of agreement held for the  $\frac{1}{2}$  in. dia cases as well.

*Dissipation and shear stress measurements*

Figure 10 shows some of the shear stress measurements. The distinctive feature that was

observed in the shear stress measurement was the abrupt change in sign that occurred when one traversed through the midpoint between the cylinders. Another feature was the dependence on the sign of the velocity gradient. This type of flow situation also points out the basic defect of Prandtl's mixing length hypothesis

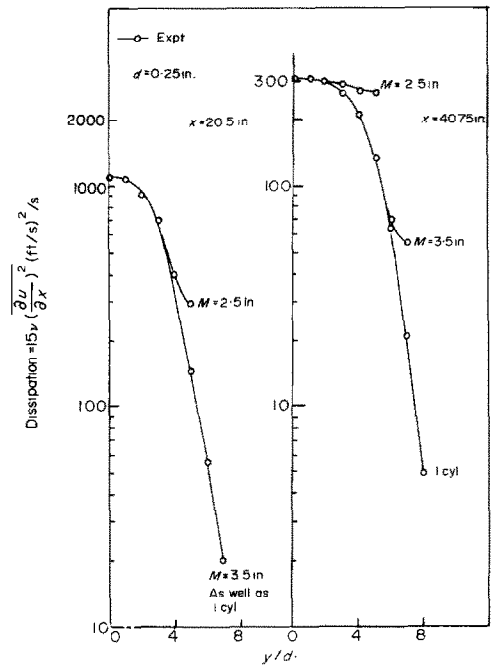


FIG. 11. Dissipation profiles.

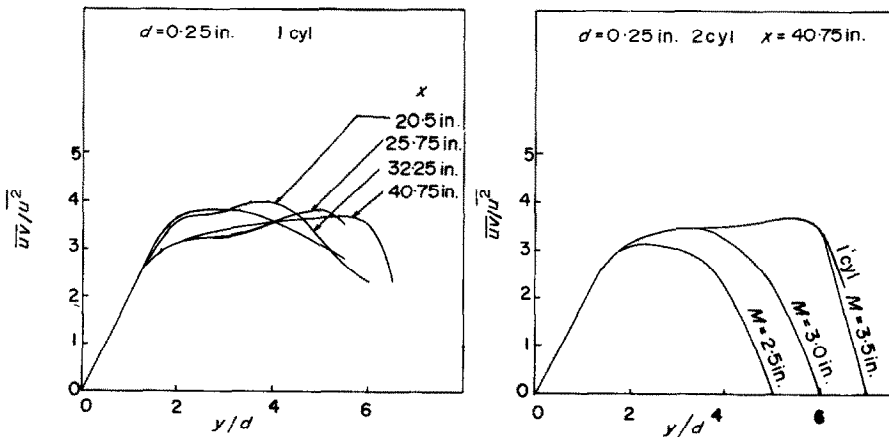


FIG. 10.  $\bar{u}'v'$  profiles.

where even though the shear stress may be zero there is considerable turbulent mixing taking place.

The measurements of dissipation are shown in Fig. 11. From these the micro or dissipation scale of turbulence has been calculated

$$\lambda^2 = \bar{u}^2 \left( \frac{du}{dx} \right)^2.$$

This is shown in Figs. 12 and 13. In these two figures, the concept of the virtual origin,  $x_0$ , (Ref. [8] for details) has been used to check if the profile of microscale of turbulence across the

wake for different diameter cylinders can be made to collapse to a single curve. The value of  $x_0$  was chosen by trial. The single cylinder as well as two cylinder cases are shown on the same graphs. At  $x = 20.5$  in.,  $\lambda$  has a constant value of about 0.09 in. for almost the entire width of the wake. A similar plot for  $x = 40.75$  in. shows a little more scatter but the general characteristics are the same. The average value of  $\lambda$  at  $x = 40.75$  in. is 0.12 in. Even for  $M = 2.5$  in.,  $d = 0.25$  in. where there is strong interaction between the wakes, the small scale structure of the turbulence seems unaffected.

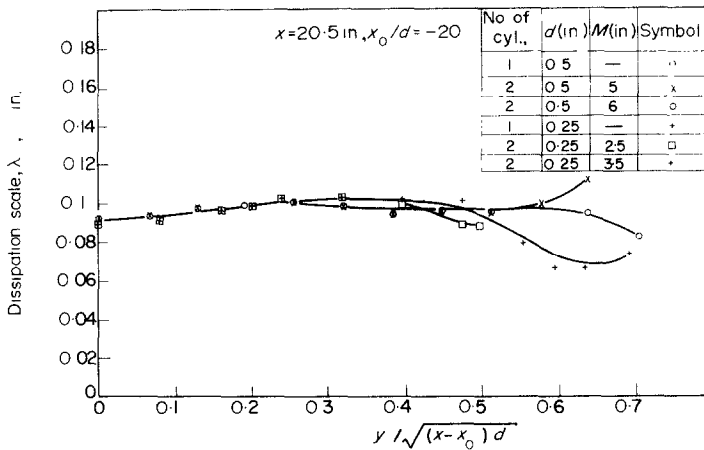


FIG. 12. Dissipation scale ( $x = 20.5$  in.,  $x_0/d = -20$ ).

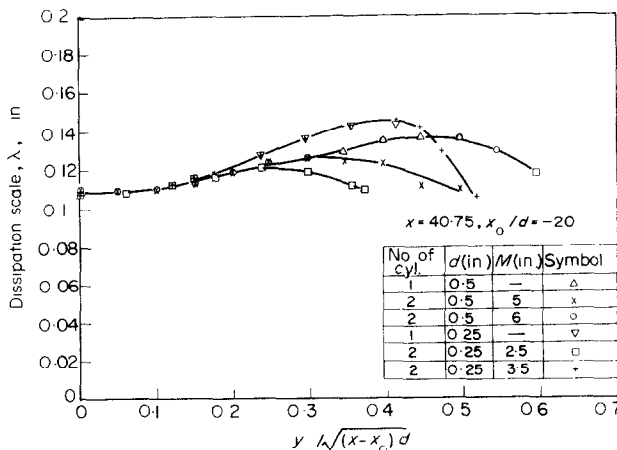


FIG. 13. Dissipation scale ( $x = 40.75$  in.,  $x_0/d = -20$ ).

With the measured values it is possible to compute the length scale used in Prandtl-Kolmogorov model of shear stress. By definition,

$$\tau = \rho \overline{uv} = \mu_{\text{eff}} \frac{\partial U}{\partial y}$$

For the Prandtl-Kolmogorov model

$$\mu_{\text{eff}} = \rho l_k (\overline{q^2})^{\frac{1}{2}}$$

therefore

$$\overline{uv} = l_k (\overline{q^2})^{\frac{1}{2}} \frac{\partial U}{\partial y}$$

or

$$l_k = \frac{\overline{uv}}{(\overline{q^2})^{\frac{1}{2}} \frac{\partial U}{\partial y}}$$

For  $d = 0.25$  in.,  $x = 40.75$  in. this was calculated at  $y = 1$  in. from the centreline of the cylinder. This gave an experimental value of  $l_k = 0.101$  in.  $\pm 15$  per cent. In theoretical methods using the Prandtl-Kolmogorov model the length scale is defined as equal to  $\lambda b$  where  $\lambda = 0.6$ , an empirical constant, and  $b$  is the half width of the wake. In the present case this worked out to  $0.124$  in. The measured dissipation scale was  $0.12$  in.

*Turbulent kinetic energy balance*

The TKE equation can also be written in the following nondimensional form [7]

$$\begin{aligned} \frac{\partial}{\partial X} \frac{\overline{q^2}}{U_{FS}^2} + \frac{\partial}{\partial Y} \frac{1}{U_{FS}^3} v \left( \frac{p}{\rho} + \overline{q^2} \right) \\ + \frac{\overline{uv}}{U_{FS}^2} \frac{\partial}{\partial Y} \frac{U_d}{U_{FS}} \\ + \frac{15\nu}{dU_{FS}} \frac{\partial}{\partial x} \left( \frac{u}{U_{FS}} \right)^2 = 0 \end{aligned} \quad (12)$$

where  $X = x/d$  and  $Y = y/d$ . The first term represents convection of TKE, the second diffusion, the third production and the fourth term is turbulent dissipation. The quantities needed to evaluate all the terms except diffusion

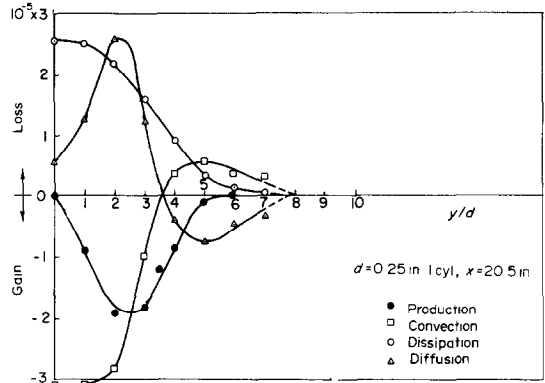


FIG. 14. TKE balance.

have been measured and diffusion has been obtained by difference from equation (12). These are shown in Figs. 14-17. The general shape of the distribution of the various terms across the wake in the single cylinder seems to be well established. There could be considerable error when one considers them quantitatively due to the large gradients of some of the terms like  $\overline{uv}$  and  $\partial U/\partial y$ . However various trends are less subject to error.

Townsend in his numerous papers on the 2-D wake has discussed the structure of single cylinder wakes. In the case of two cylinders, due to the interaction of the wakes, certain effects can be observed. These are mainly on the convection, dissipation and diffusion terms. The

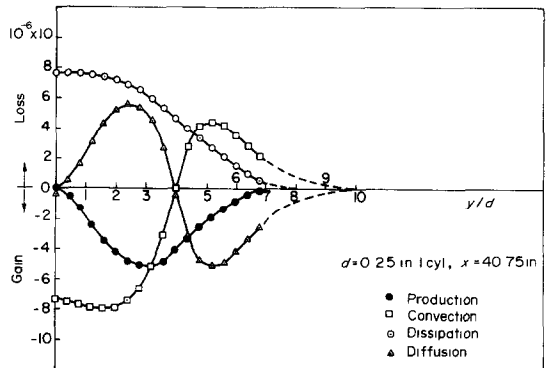


FIG. 15. TKE balance.

production term seems the least affected by wake interaction.

Near the axis of the wake the main contributions are due to convection and dissipation. There is some diffusion. The effect of convection here would be to increase TKE and the other two terms decrease TKE. At  $y/d \approx 0.4$  convection and diffusion are nearly absent and production is balanced by dissipation. Up to this point the single and multiple wakes seem similar. As we move towards the edge of the wake, in the one cylinder case production and dissipation fall rapidly to zero. The main contributions are due to convection and diffusion. The sign of the

convection term is changed and it tends to decrease TKE in this region. In the two cylinder case the contribution from convection is reduced. However, the contribution due to dissipation and diffusion are markedly increased.

*Accuracy of measurements*

Accuracy has been discussed in detail in [13]. The main points will be mentioned here. The maximum error in the measurement of turbulent kinetic energy has been estimated to be about 8 per cent. In the case of shear stress the error is of the order of  $\pm 8$  per cent. It is difficult to estimate the error in the measurement of

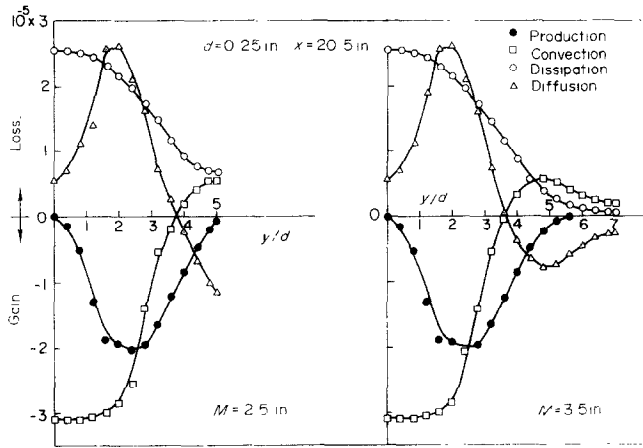


FIG. 16. TKE balance.

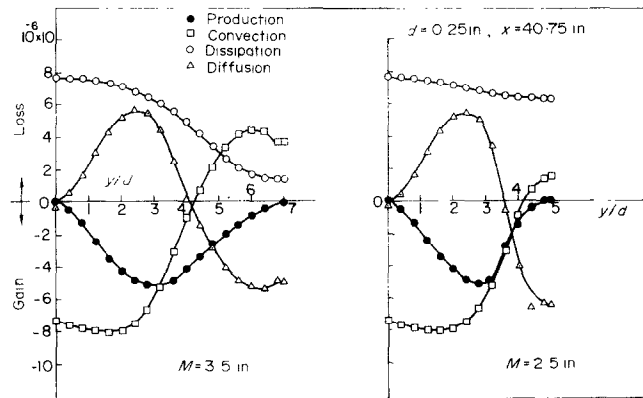


FIG. 17. TKE balance.

dissipation. It is not resolved to what degree of accuracy, the concepts of Taylor's hypothesis and local isotropy are valid in shear flows. Lacking this information, one can only estimate the error in dissipation from a knowledge of the integrated diffusion in the case of single cylinder wakes. This value should be theoretically zero. In the present measurements there was an average residual integrated value of diffusion of about 12 per cent of the sum of integrated values of production and convection. The uncertainties in the measurement of intermittency have been discussed in [12]. The maximum error could be of the order of  $\pm 12$  per cent depending on the location of measurement. This error is mainly due to problem of calibrating the intermittency circuit. Near the centreline of the wake and the edge of the wake, the uncertainty reduces to about  $\pm 2$  per cent.

#### CONCLUSIONS

The main conclusions are that surprisingly simple formulations can be used successfully in predicting some of the features in interacting wakes based on measurements in single cylinder wakes. It remains to be seen how valid these formulations will be when applied to other types of interacting shear flows.

Wake interaction seems to affect the various terms in the TKE equation at different rates. Dissipation and diffusion are the first to be affected. They both increase. Convection is affected next. The ability to convect TKE away from the zone of interaction is reduced as interaction proceeds. The production term is the last to be affected. It is reduced.

#### MESURE DE TURBULENCE DANS DES SILLAGES EN INTERACTION

**Résumé**—On a fait des mesures détaillées de grandeurs de turbulence dans le sillage d'interaction de deux cylindres. Les mesures comprennent les profils de vitesse moyenne, l'énergie cinétique de turbulence, la contrainte tangentielle de Reynolds, l'intermittence et la dissipation dans le sillage de deux cylindres d'égal diamètre pour plusieurs distances en aval. On a fait varier les diamètres des cylindres aussi bien que leur espacement. De simples formulations ont été faites pour estimer l'intermittence et l'énergie cinétique dans les sillages de deux cylindres, basées sur le sillage d'un cylindre unique. Une comparaison avec les profils mesurés est satisfaisante. Les termes individuels de l'équation d'énergie cinétique de turbulence ont été évalués pour présenter le bilan de l'énergie cinétique de turbulence. Les mesures ont été effectuées à 26 m/s et correspondent à un domaine de nombre de Reynolds entre 11000 et 22000 (basé sur le diamètre d'un seul cylindre).

#### ACKNOWLEDGEMENTS

The authors would like to acknowledge with thanks the financial support of the National Research Council and the Defense Research Board of Canada for this project. One of us (BVS) was also the recipient of the Province of Ontario Graduate Fellowship (1970–71) which is gratefully acknowledged.

#### REFERENCES

1. R. GRAN OLSSON, Geschwindigkeits- und Temperaturverteilung hinter einem Gitter bei turbulenter Stromung, *Z. Angew. Math. Mech.* **16**, 257–274 (Oct. 1942).
2. H. TAMAKI and K. OSHIMA, Experimental studies on the wake behind a row of heated parallel rods, Proc. 1st Japan National Congress of Applied Mechanics, 459–463 (1951).
3. H. SATO, On the turbulence behind a row of heated parallel rods, Proc. 1st Japan National Congress of Applied Mechanics, 469–475 (1951).
4. R. W. STEWART, An experimental study of homogeneous and isotropic turbulence, Ph.D. thesis, University of Cambridge (1951).
5. R. KNYSTAUTAS, The turbulent jet from a series of holes in line, *Aero Q.* **XV**, 1–28 (Feb. 1964).
6. F. H. CHAMPAGNE and I. J. WYGNANSKI, An experimental investigation of coaxial turbulent jets, *Int. J. Heat Mass Transfer* **14**, 1445–1464 (1971).
7. J. O. HINZE, *Turbulence*. McGraw-Hill, New York (1959).
8. A. A. TOWNSEND, *The Structure of Turbulent Shear Flow*. Cambridge University Press (1956).
9. L. J. S. BRADBURY, The structure of a self-preserving turbulent plane jet, *J. Fluid Mech.* **23**, 31–64 (1966).
10. S. C. KACKER and J. H. WHITELAW, The turbulent characteristics of two dimensional wall jet and wall wake flows, *J. Appl. Mech.* **38**, 239–252 (1971).
11. S. CORSSIN and A. L. KISTLER, Free stream boundaries of turbulent flows, NACA TN No. 3133 (1954).
12. B. V. SESHAGIRI and G. M. BRAGG, Uncertainty in measurement of intermittency in turbulent free shear flows, *AIAA J* **10**, 542–543 (1972).
13. B. V. SESHAGIRI, Properties of turbulent interacting wakes, Ph.D. thesis, University of Waterloo, Canada (1971).
14. G. M. BRAGG, H. S. KOHLI and B. V. SESHAGIRI, Mean flow calculations behind arbitrarily spaced cylinders, *J. Basic Engng* **92**, 536–543 (1970).
15. J. L. GRANT, The large eddies of turbulent motion, *J. Fluid Mech.* **4**, 149–190 (1958).

## TURBULENZMESSUNGEN BEI SICH ÜBERLAGERNDEN NACHLAUFSTRÖMUNGEN

**Zusammenfassung**—Detaillierte Messungen von turbulenten Grössen wurden im Nachlauf zweier Zylinder gemacht. Die Messungen umfassen die Profile der mittleren Geschwindigkeit, der kinetischen Energie bei Turbulenz, der Reynolds-Scherspannung, der Intermittenz und der Dissipation im Nachlauf zweier Zylinder mit gleichem Durchmesser, an einer Reihe von Stellen stromabwärts. Abstand und Durchmesser der Zylinder wurden variiert. Es wurden einfache Ansätze gemacht, um die Verteilung der Intermittenz und der kinetischen Energie bei Turbulenz im Nachlauf zweier Zylinder zu bestimmen, auf Grund von Messungen hinter einem Einzelzylinder. Der Vergleich mit den gemessenen Profilen zeigte zufriedenstellende Übereinstimmung. Die besonderen Ausdrücke für die turbulente kinetische Energie wurden entwickelt, um die TKE-Bilanz darzustellen.

Die Messungen wurden bei 26 m/s gemacht, was einem Bereich der Reynoldszahlen von 11 000 bis 22 000 entspricht (bezogen auf den Durchmesser eines Einzelzylinders).

## ИЗМЕРЕНИЯ ТУРБУЛЕНТНОСТИ ПРИ ВЗАИМОДЕЙСТВИИ СПУТНЫХ СТРУЙ ЗА ЦИЛИНДРАМИ

**Аннотация**—Проведены подробные измерения характеристик турбулентности при взаимодействии спутных струй за двумя цилиндрами. При измерениях находились профили средней скорости, энергия пульсационного движения, напряжение Рейнольдса, перемежаемость и диссипация при взаимодействии спутных струй за цилиндрами одинаковых диаметров в различных точках вдоль по потоку. Диаметры цилиндров, а также расстояние между ними изменялись. Предложены простые формулы для расчета распределения перемежаемости энергии пульсационного движения в спутных струях за двумя цилиндрами на основании измерений следа за одним цилиндром. Сравнение этих расчетов с измеренными профилями показало удовлетворительное соответствие. Были рассчитаны отдельные члены уравнения баланса энергии пульсационного движения.

Измерения проводились при скорости 87 фут/сек, что соответствовало диапазону чисел Рейнольдса 11000–22000 (рассчитанных по диаметру одиночного цилиндра).